



## Fabrication and characterization of IC-Compatible Linear Variable Optical Filters with application in a micro-spectrometer

A. Emadi<sup>a,\*</sup>, H. Wu<sup>a</sup>, S. Grabarnik<sup>a</sup>, G. De Graaf<sup>a</sup>, K. Hedsten<sup>b</sup>, P. Enoksson<sup>b</sup>, J.H. Correia<sup>c</sup>, R.F. Wolffenbuttel<sup>a</sup>

<sup>a</sup> Faculty of EEMCS, Department for ME/EI, Delft University of Technology, Delft, The Netherlands

<sup>b</sup> MC2, Chalmers University of Technology, SE-412 58 Gothenburg, Sweden

<sup>c</sup> Department of Industrial Electronics, Campus de Azurém, University of Minho, 4800-058 Guimarães, Portugal

### ARTICLE INFO

#### Article history:

Received 15 October 2009

Received in revised form 23 March 2010

Accepted 12 April 2010

Available online 7 May 2010

#### Keywords:

Linear variable filter

Micro-spectrometer

Tapered layer

Reflow

Optical filter

Thin film

### ABSTRACT

This paper reports on an IC-Compatible process for the fabrication of Linear Variable Optical Filter (LVOF). The LVOF is integrated with a detector array to result in a micro-spectrometer. The technological challenge in fabrication of an LVOF is fabrication of a well-controlled tapered cavity layer. Very small taper angles, ranging from  $0.001^\circ$  to  $0.1^\circ$ , are fabricated in a resist layer by just one lithography step and a subsequent reflow process. The 3D pattern of resist structures is subsequently transferred into  $\text{SiO}_2$  by an appropriate etching. Complete LVOF fabrication involves CMOS-compatible deposition of a lower dielectric mirror using a stack of dielectrics on the wafer, tapered layer formation and the deposition of the top dielectric mirror. The design principle, IC-Compatible processing and the characterization results on fabricated LVOFs are presented.

© 2010 Elsevier B.V. All rights reserved.

### 1. Introduction

Single-chip optical micro-spectrometers have huge potential in many applications, such as identification of bio-molecules, gas detection and in chemical analysis, because of their properties such as low-cost and low sample volume [1–5]. A small Linear Variable Optical Filter (LVOF) integrated with an array of optical detectors is a very suitable candidate for a micro-spectrometer that should feature both low unit cost and high resolving power [6,7]. Although grating-based micro-spectrometers generally outperform optical resonance based systems, such as the Fabry–Perot etalon or the LVOF-based micro-spectrometer, in case of operation over a wide spectral bandwidth, LVOF-based micro-spectrometers are more suitable for operation with high resolving power over a narrow spectral band, as is required in spectral analysis around an absorption line [8]. IC-Compatible fabrication enables the fabrication of LVOFs as a post-process in CMOS. Having the detector array and electronic circuits realized in CMOS prior to application of the post-process offers opportunities for low unit costs in case of a high production volume.

The LVOF is basically a one-dimensional array of many Fabry–Perot (FP)-type of optical resonators. Rather than a huge number of discrete devices [9], the LVOF has a center layer (the resonator cavity) in the shape of a strip and a thickness that changes over its length. Dielectric mirrors are on either side. The spectral resolution of a Fabry–Perot interferometer is determined by surface flatness, parallelism between the two mirror surfaces and mirror reflectivity. The possibility to have high number of spectral channels in an LVOF spectrometer theoretically makes it possible to have spectral resolution better than 0.2 nm in the visible spectrum range using signal processing techniques. For a Fabry–Perot type of LVOF, the thickness variation of the cavity layer has to be in order of quarter of the wavelength and very well controlled, which makes fabrication of miniature LVOFs a technological challenge. The theoretical limit for the spectral resolving power of the LVOF-based spectrometer is the spectral bandwidth divided by the number of channels in the detector array. However, this is difficult to achieve when considering the signal to noise ratio. This simple geometric optimum is only approached in case of a high SNR.

LVOF fabrication is based on reflow of a specially patterned layer of resist. Fig. 1 shows the process steps for the fabrication of an IC-Compatible LVOF. The process starts by deposition of the lower dielectric mirror stack and the oxide layer that results in the cavity layer. Photoresist is spin coated as the next step and lithography is applied to define the strip-like structure in the resist layer to be

\* Corresponding author.

E-mail address: [arvin.emadi@gmail.com](mailto:arvin.emadi@gmail.com) (A. Emadi).

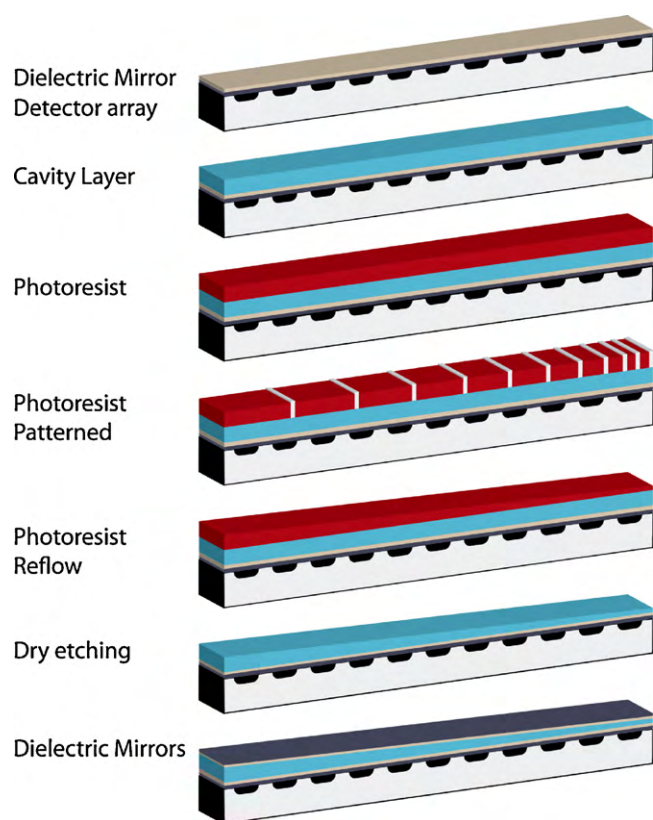


Fig. 1. Process flow for the fabrication of LVOF.

reflowed. A series of trenches of constant width and with variable spatial frequency or trenches of variable width and constant pitch are etched over the length of the strip to vary the effective amount of resist per unit area. The subsequent reflow transfers this gradient volume of resist into a smooth tapered resist layer. The topography of the tapered resist layer is transformed into the thick oxide cavity layer by an appropriate plasma etching process. The process is completed by deposition of the top dielectric mirror stack. This first prototype of the LVOF is fabricated on a glass substrate. However, fabrication directly on a CMOS detector chip as a compatible post-process is well possible.

For the LVOF presented in this work the wavelength range of 570–720 nm is chosen. This wavelength range contains the essential information in applications such as fluorescence spectroscopy of plants and H- $\alpha$  spectroscopy. The performance characterization of the LVOF and related micro-spectrometer in this wavelength range can be tested using a Neon lamp, which has most of its major peaks in this wavelength range. The same principle of design can be applied to other wavelength ranges in visible, Infrared and UV. The difference would be the choice of dielectric materials for the LVOF filter and suitable detector array. For near-infrared region, for example PolySi and SiO<sub>2</sub> are to be used as dielectric materials [10] and MEMS fabricated thermopile arrays as detectors [11].

## 2. Design and fabrication

The dielectric multilayered Fabry–Perot LVOF consists of 14 alternative layers of TiO<sub>2</sub> and SiO<sub>2</sub>. Table 1 shows the layers thicknesses required for a visible LVOF to cover the 570–720 nm spectral range based on optical simulations. Fig. 2 shows the simulated spectral response for different thicknesses of the cavity layer, which gives a prediction of the spectral response of the LVOF at different positions along its length. As the table shows, the cavity

**Table 1**  
Layers thickness for an LVOF for 570–720 nm wavelength range.

Layer material	Layer thickness (nm)
TiO <sub>2</sub>	67
SiO <sub>2</sub>	112
TiO <sub>2</sub>	67
SiO <sub>2</sub>	112
TiO <sub>2</sub>	67
SiO <sub>2</sub>	112
TiO <sub>2</sub>	67
SiO <sub>2</sub>	850–1000
TiO <sub>2</sub>	67
SiO <sub>2</sub>	112
TiO <sub>2</sub>	67
SiO <sub>2</sub>	112
TiO <sub>2</sub>	67
SiO <sub>2</sub>	112
TiO <sub>2</sub>	67
SiO <sub>2</sub>	112

layers thickness should vary between 850 nm and 1000 nm to cover the desired wavelength range. The simulation has been done with TFCalc<sup>®</sup> 3.3 software [12]. The spectral bandwidth of the filter depends on reflection spectrum of dielectric mirrors and the order of the Fabry–Perot. Increasing the order of the cavity results in higher resolving power, but limits the operating free spectral range of Fabry–Perot etalon. The LVOF based on the Fabry–Perot etalon listed in Table 1 gives a half-power spectral bandwidth HPBW=2.2 nm over 150 nm wavelength range. The HPBW of an LVOF is slightly larger than that of a corresponding Fabry–Perot, because of multiple reflections between the non-parallel mirrors [13].

Based on the simulation it was decided to design for 2 types of LVOFs; the first with a length of 2.5 mm and the second with a length of 5 mm. In the 5 mm long LVOF the thickness variation (slope) would be equal to 150 nm/5 mm. In case collimated light of a single wavelength is used to illuminate the strip, the light over a small length is transmitted, due to filtering property of the LVOF. The length of the transmitted light spot can be calculated as:  $\Delta x = \text{HPBW}/\theta$ , where  $\theta$  denotes the slope of the LVOF. Using the values of HPBW = 2.2 nm and above-mentioned slope angle results in  $\Delta x \approx 75 \mu\text{m}$ . This means for each single wavelength in the spectrum a region of 75  $\mu\text{m}$  in length is illuminated on the detector. Therefore, if a typical detector with 5  $\mu\text{m}$  pitch is used, about 15 pixels on the detector are illuminated.

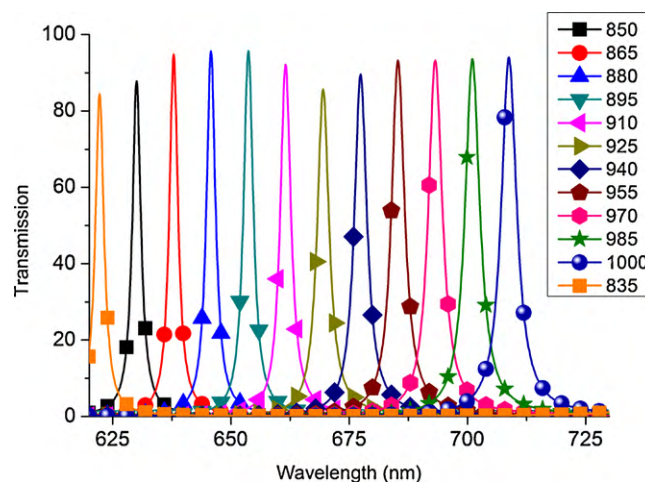


Fig. 2. Simulated spectral response of multilayered Fabry–Perot for different cavity layer thicknesses, thickness values in nm.

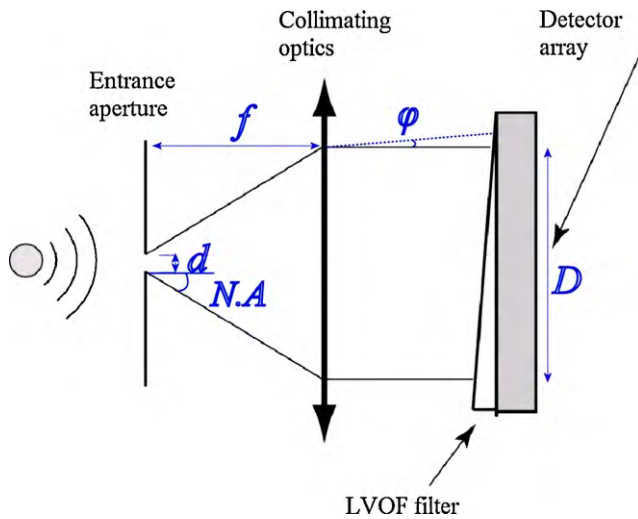


Fig. 3. Structure of LVOF micro-spectrometer.

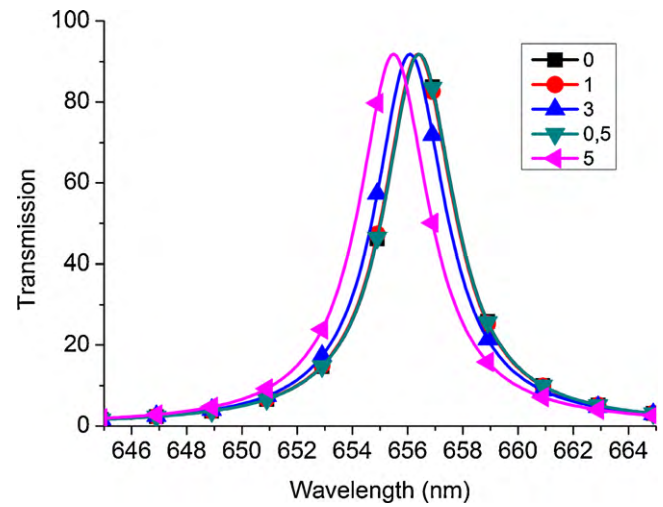


Fig. 4. Transmission through the multilayered Fabry–Perot at different angles.

The structure of an LVOF-based micro-spectrometer is shown in Fig. 3. Light passes an aperture and collimating optics before being projected onto the LVOF, which is placed or deposited on the top of the detector. The entrance aperture in Fig. 3 can be larger than that typically used in grating-based micro-spectrometers, allowing more light entering the optical system. Consequently, the resolution of the micro-spectrometer depends primarily on the Half-Power BandWidth (HPBW) of the LVOF, rather than on the aperture size. To determine the size of aperture and focal length of the collimating lens the following equations can be used.

Fig. 3 results  $f = D/2NA$ , in which  $D$  is size of the LVOF,  $f$  is the focal length of the lens and  $NA$  is entrance numerical aperture. Smith–Helmholtz invariant theorem [14] results  $d \cdot NA = D \cdot \phi$ , that can be rewritten as  $d = D \cdot \phi / NA$  in which  $d$  is the diameter of the aperture and  $\phi$  is maximum acceptable angle of incidence on the LVOF. Since these equations depend on  $\phi$ , transmission through the multilayered Fabry–Perot filter (which can be at any position along the length of the LVOF) is simulated at different angles. Fig. 4 shows the result. It can be seen that at  $3^\circ$  angle of incident there is 0.4 nm wavelength shift in the spectral response and at  $5^\circ$  angle of incident this wavelength shift has increased to 0.9 nm. Based on these simulations  $\phi$  can be selected. For spectral accuracy better than 2 nm,  $\phi = 5^\circ$  is an acceptable choice.

The first step for the fabrication of LVOF is to deposit dielectric mirrors, layers 1–7, and a thick oxide of 1050 nm, layer 8, on a 4 in. glass wafer. The thick oxide layer is tapered in subsequent process steps. A FHR MS 150 sputter machine has been used for the deposition of  $TiO_2$  and  $SiO_2$  films.  $TiO_2$  is deposited by reactive DC sputtering and  $SiO_2$  by reactive RF sputtering. The films can be deposited subsequently without breaking the vacuum. The films are optically characterized by ellipsometry and the data were used to refine the values used for the designed thicknesses. The thickness variation over the 4 in. wafer size is measured to be less than 2% for both films. The effect of such a relative thickness is shown in the simulation of reflectance of the optical filter, as shown in Fig. 5. Thickness variation can cause  $\pm 6$  nm wavelength shift of the peak. This implies that fabricating a Fabry–Perot at an exact desired peak can be challenging. However, for an LVOF type of Fabry–Perot this problem is resolved since the sloped cavity layer makes it possible to cover the whole spectrum range of interest despite of wavelength shift. The 4 in. glass wafer is diced into  $2\text{ cm} \times 2\text{ cm}$  pieces before applying further processing.

The  $SiO_2$  cavity layer is tapered in an IC-Compatible fabrication process. Initially, a tapered photoresist layer is formed by one step lithography and reflow of the resist. Subsequently, the topography of the tapered resist layer is transferred into  $SiO_2$  by RIE. With a single lithography step a pattern of trenches (or holes) is developed

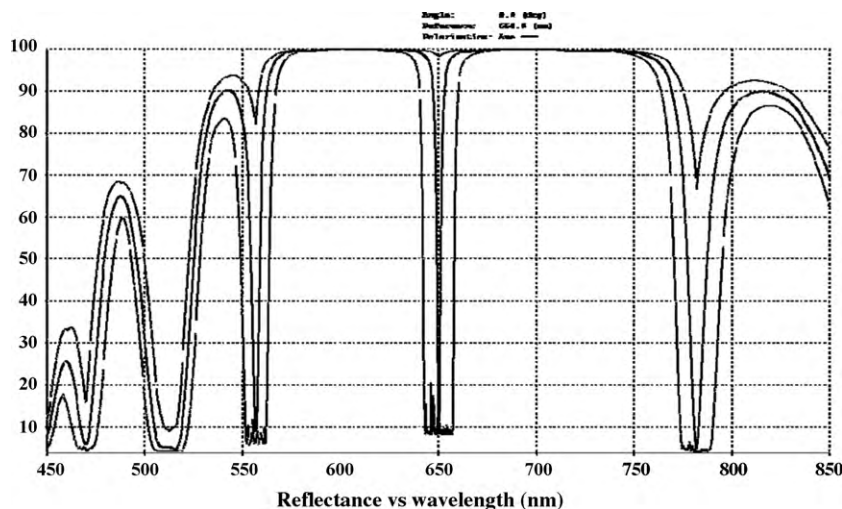


Fig. 5. Simulated reflectance spectrum of multilayered Fabry–Perot for 850 nm thickness of the cavity layer.

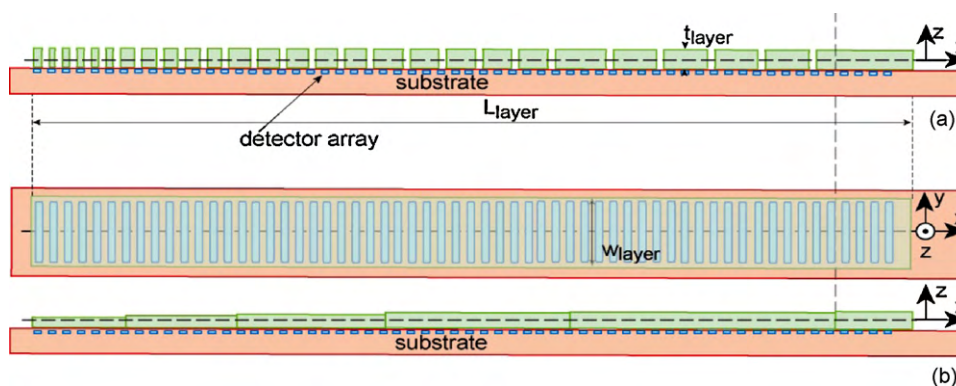


Fig. 6. (a) Pattern of trenches in the photoresist layer. (b) Tapered resist layer after reflow.

in a photoresist layer. The trench or holes size is  $2\ \mu\text{m}$ , which is the minimum possible with the available lithography. The trench density defines the local amount of material removed (Fig. 6a) and is followed by reflow of this patterned photoresist to locally planarize the remaining strips of material (Fig. 6b). The result is an effective reduction of the resist layer thickness by a value defined by localized trench density. Hence a taper can be flexibly programmed by mask design to be from  $0.001^\circ$  to  $0.1^\circ$ . This enables simultaneous fabrication of tapered layers of different angles. The mask is designed based on a geometrical model and FEM simulations using COMSOL [15].

Two different types of photoresist have been used in the fabrication: AZ4562 and Shipley S1813. AZ4562 has an initial thickness of  $4\text{--}4.5\ \mu\text{m}$  after spin coating. S1813 is a thinner resist with initial thickness of  $1.2\ \mu\text{m}$  after spin coating and is used in fabrication of smaller slopes.

The viscosity of the resist decreases rapidly at temperatures above the glass transition temperature and the material flows because of surface tension, while remaining coherent. Although the glass transition temperature of resist is relatively low value ( $110\text{--}120^\circ\text{C}$ ), the resist does not flow well over the substrate due to its high viscosity. Another approach to decrease the viscosity of the resist is to expose it to its solvent vapor. The wafer with patterned photoresist is alternatively exposed for short time to solvent, so that the resist absorbs some of the solvent vapor and is subsequently exposed to a temperature above glass transition temperature until most of the solvent is removed. Cross-linking of the resist is avoided and a better control on the quality of the surface is obtained. A process has been designed with a limited number of solvent exposure/baking cycles and optimized towards minimum surface roughness for the desired range of taper angles. The samples with patterned resist on the dielectric stack are exposed to PGMEA solvent vapor heated to  $50^\circ\text{C}$  for 3 h and heated on hot-plate at  $110^\circ\text{C}$  for 10 min. Fig. 7 shows profile scans on tapered

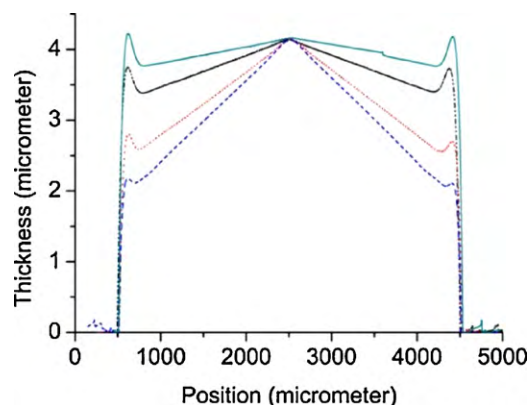


Fig. 7. Profiles of four 4 mm long tapered resist structures.

AZ4562 resist layers. It can be seen that different slopes with the same initial thickness have been fabricated and the profile of the structures is smooth.

The process for transferring the resist structure into  $\text{SiO}_2$  is optimized to get an optically smooth surface. The process uses a mixture of  $\text{NF}_3$  5 sccm, Ar 50 sccm and  $\text{O}_2$  30 sccm at 20 mTorr with 100 W. The etch rate of  $\text{SiO}_2$  is  $0.7\ \text{nm/s}$  and etch rate of the resist is  $4.6\ \text{nm/s}$  which gives a resist/ $\text{SiO}_2$  etch ratio of 6.5. A laser illuminates the thickest part of the resist structure during etching and the reflection from the surface is measured. Due to interference between resist, oxide layer and substrate, this will show exactly how much of the resist and  $\text{SiO}_2$  has been etched. The etching process is stopped after resist is removed from the thickest part and 50 nm of the  $\text{SiO}_2$  under it, is etched. Fig. 8a and b shows the video screen of the etching system before and during the etching. The dark and light strip pattern on the resist structure illustrates the slope shape. In Fig. 8b

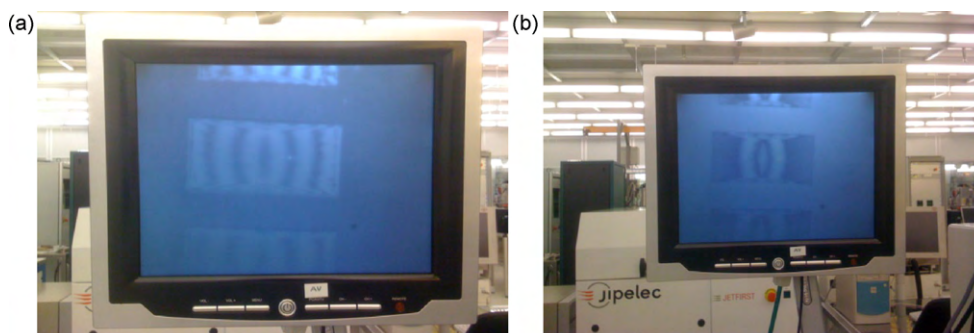


Fig. 8. Patterns, due to interference, illustrate the sloped shape of the structures: (a) before start of etching and (b) during etching.



Fig. 9. LVOF deposited on the glass mounted at the entrance of the Camera. The glass contains five different LVOF filters.

resist has been etched from the thin part of the resist structure and etching of the  $\text{SiO}_2$  has started in those areas.

After etching the samples are cleaned in acetone and further by oxygen plasma to remove any remaining of photoresist. Sub-

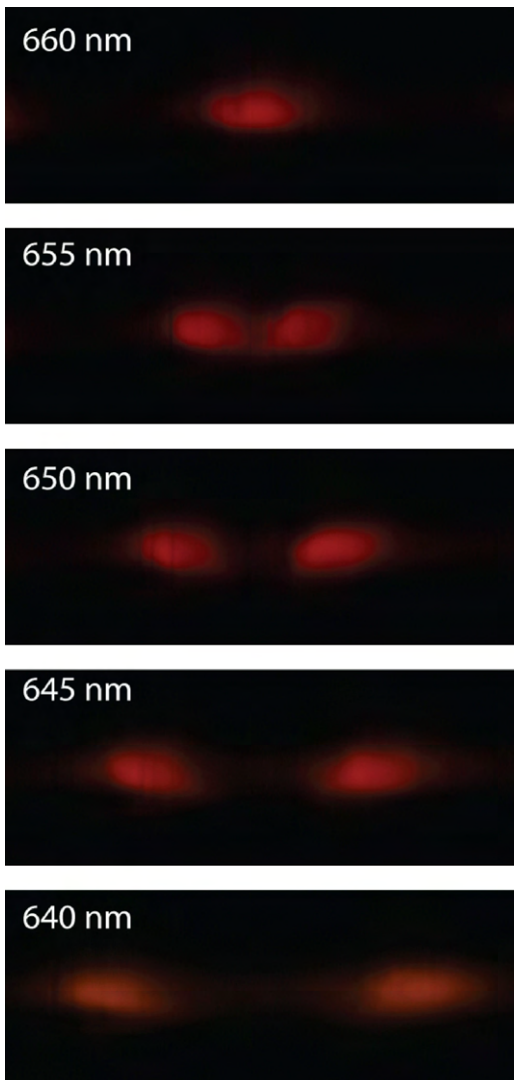


Fig. 10. Image recorded on the CCD at several wavelengths.

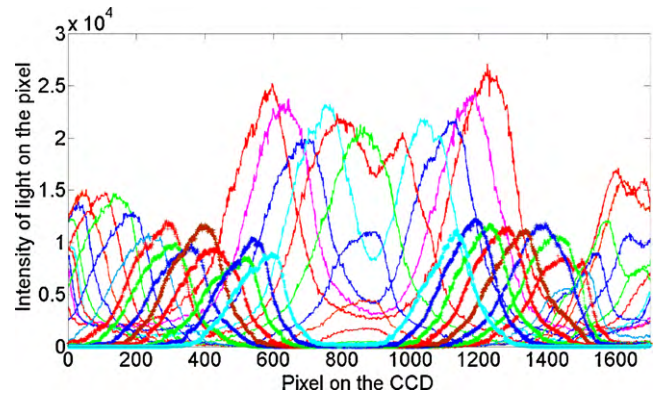


Fig. 11. Intensity of light recorded on the CCD at several wavelengths (580–720 nm).

sequently, the dielectric stacks, layers 9–16 from Table 1, are deposited on the samples to complete the LVOFs.

### 3. Characterization

Characterization involves illumination of the LVOF with monochromatic light and recording the image due to transmission through the LVOF using a CCD. The wavelength of the monochromatic light is swept over the wavelength range of the LVOF. A Canon EOS 10D camera has been used for the characterization of the LVOF filter. Fig. 9 shows the LVOF placed on the entrance of the Canon camera. Infrared blocking filter of the camera has been removed. Collimated monochromatic light is projected on the LVOF and the wavelength of light is swept with 1 nm steps. The image recorded on the Camera is exported to Matlab®. There is 3 cm distance between the LVOF and the camera. This has an adverse effect on the quality of the projected image and thus on the measurements, because of the diverging light.

Fig. 10 shows image on the camera at several wavelengths. The illuminate part moves along the detector as the wavelength is swept. The illuminated strip is around 1 mm, which is a much larger spot size than the calculated  $75 \mu\text{m}$  strip size. This is directly due to the distance between the LVOF and the detector. It can be easily calculated that a  $1^\circ$  diverging angle causes a 1 mm area spot size in case of a 3 cm distance. Fig. 11 shows the intensity of the pixel on the camera at different wavelengths. The wavelength is swept from 580 nm to 720 nm. For each monochromatic wavelength around 200 of the pixel on the CCD are illuminated. This is

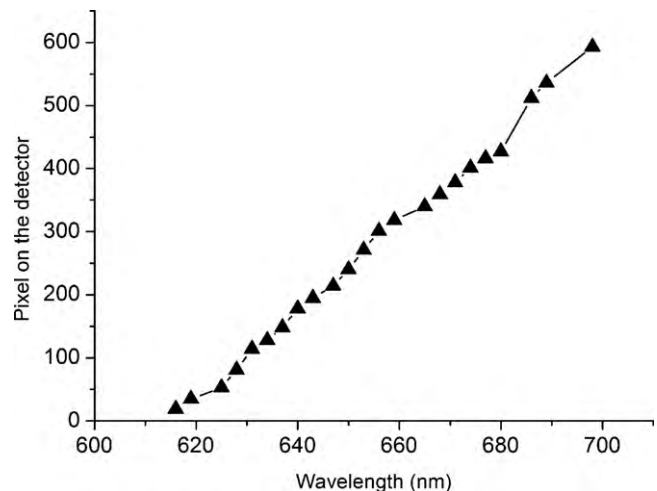


Fig. 12. Position of transmission peak along the LVOF.

mainly due to the distance between LVOF and detector and partly due to bandwidth of the monochromatic light and HPBW of the LVOF at each position. The position of illuminated pixels on the CCD shifts over about 30 pixels per 3 nm wavelength, which is equivalent to 10 pixels/nm. This characterization data can be used for the calibration of the spectrometer [16,17]. The shift over a large number of pixels is a desirable property for high-resolution spectral measurements after calibration. Fig. 12 shows the position of the intensity peaks on the detector versus wavelength. This figure shows that the wavelength of the light passing through the LVOF changes linearly with the position along the length of the LVOF. Placing the LVOF directly on the top of a linear detector array in CMOS in a CMOS-compatible fashion strongly reduces the problems associated with diverging light mentioned. Also the use of characterization data for calibration and spectral measurements is subject of future work.

#### 4. Conclusions

LVOFs for operation in a wavelength range between 570 nm and 720 nm have been fabricated with an IC-Compatible process. The process includes a reflow process to fabricate a smooth tapered layer in resist. Miniature LVOFs fabricated by this technique can be used for mass production of on-chip micro-spectrometers. Characterization of the LVOFs using monochromatic light proves the operation for the LVOF. Spectral measurements using the LVOF are possible after using the characterization data to calibrate the wavelength response. Future research is directed towards a fully integrated micro-spectrometer in CMOS.

#### Acknowledgements

This work has been supported by the Dutch Technology Foundation STW under grant DET.6667. Parts of this work have been done in Nano-Fabrication Laboratory at MC2, Chalmers University of Technology with support from the EU funded MC2ACCESS programme. The authors would like to thank H. Frederiksen and M. Hagberg for their support with sputtering and RIE tools.

#### References

- [1] G. Minas, R.F. Wolffenbuttel, J.H. Correia, An array of highly selective Fabry–Perot optical channels for biological fluid analysis by optical absorption using a white light source for illumination, *J. Opt. A: Pure Appl. Opt.* 8 (2006) 272–278.
- [2] J.C. Ribeiro, G. Minas, P. Turmezei, R.F. Wolffenbuttel, J.H. Correia, A SU-8 fluidic microsystem for biological fluids analysis, *Sens. Actuators A* 123–124 (2005) 77–81.
- [3] G. Minas, R.F. Wolffenbuttel, J.H. Correia, A lab-on-a-chip for spectrophotometric analysis of biological fluids, *RSC Lab Chip*, 5 (11) (2005) 1303–1309.
- [4] S. Grabarnik, R.F. Wolffenbuttel, A. Emadi, M. Loktev, E. Sokolova, G. Vdovin, Planar double-grating micro-spectrometer, *Opt. Express* 15 (March (6)) (2007) 3581–3588.
- [5] L. Fonseca, R. Rubio, J. Santander, C. Calaza, N. Sabate, P. Ivanov, E. Figueras, I. Gracia, C. Cane, S. Udina, M. Moreno, S. Marco, Qualitative and quantitative substance discrimination using a CMOS compatible non-specific NDIR microarray, *Sens. Actuators B: Chem.* 141 (September (2)) (2009).
- [6] R. McLeod, T. Honda, Improving the spectral resolution of wedged etalons and linear variable filters with incidence angle, *Opt. Lett.* 30 (19) (2005) 2647–2649.
- [7] S.F. Pellicori, US Patent 4,957,371, (1990) Wedge-filter spectrometer.
- [8] S. Grabarnik, Optical microspectrometers using imaging diffraction gratings, PhD thesis, Delft University of Technology, (2010) ISBN:978-90r-r9025048-9.
- [9] R. Rubio, J. Santander, L. Fonseca, N. Sabate, I. Gracia, C. Cane, S. Udina, S. Marco, Non-selective NDIR array for gas detection, *Sens. Actuators B: Chem.* 127 (1) (2007) 69–73 (Special Issue: Eurosensors XX).
- [10] A. Emadi, S. Grabarnik, H. Wu, G. de Graaf, R.F. Wolffenbuttel, Fabrication and characterization of infra-red multi-layered interference filter, in: *Proceedings of MME 2007*, Guimaraes, Portugal, 2009, pp. 249–252.
- [11] H. Wu, S. Grabarnik, A. Emadi, G. de Graaf, R.F. Wolffenbuttel, A thermopile detector array with scaled TE elements for use in an integrated IR microspectrometer, *J. Micromech. Microeng.* 18 (2008) 064017.

- [12] TFCalc 3.3, Software Spectra Inc., 2001, <http://www.spectra.com/>.
- [13] M.A. Rob, Limitation of a wedged étalon for high-resolution linewidth measurements, *Opt. Lett.* 15 (11) (1990) 604–606.
- [14] M. Born, E. Wolf, Principles of Optics: Electromagnetic Theory of Propagation, Interference and Diffraction of Light, 7th ed., (1999) pp. 176–178.
- [15] A. Emadi, H. Wu, S. Grabarnik, G. de Graaf, R.F. Wolffenbuttel, Vertically tapered layers for optical applications fabricated using resist reflow, *J. Micromech. Microeng.* 19 (2009), 074014 (9 pp.).
- [16] O. Schmidt, P. Kiesel, M. Bassler, Performance of chip-size wavelength detectors, *Opt. Express*, 15 (15) (2007) 9701–9706.
- [17] O. Schmidt, P. Kiesel, S. Mohta, N.M. Johnson, Resolving pm wavelength shifts in optical sensing, *Appl. Phys. B* 86 (4) (2007) 593–600.

#### Biographies

**Arvin Emadi** was born in Tehran, Iran in 1982. He received Bachelor degrees in Telecommunications and Electronics from Amirkabir University of Technology (Polytechnic of Tehran) in 2003 and M.Sc. in Microwave Electronics from Chalmers University of Technology, Sweden in 2005. He joined Electronic Instrumentation Laboratory from February 2006 and he is working on micro-spectrometer project. His research interests are micro- and nano-fabrication techniques, high-Tc superconductors, IC designing and IR to UV filters and detectors.

**Huaiwen Wu** was born in Taipei, Taiwan, on May 24, 1980. He received Bachelor degree in Electrical Engineering Department from National Taipei University of Technology, Taipei, Taiwan, in 2002. After that, he served in Taiwan Marine Corps as second lieutenant in armored tank division for two years. In 2004, he worked in the design of tuner for set-up box in local electronic company. He received M.Sc. degree of Microelectronics at Delft University of Technology in 2007 and is continuing his PhD study in Electronic Instrumentation Lab. His research interests are design of Infrared Sensor System based on the thermopile using MEMS technology and CMOS-compatible optical filters.

**Semen Grabarnik** received his M.Sc. from Moscow Institute of Physics and Technology, Russia. He joined Electronics Instrumentation Lab in 2005 and finished his PhD in 2010. The title of his thesis is “Optical Microspectrometers using imaging diffraction gratings”.

**Ger de Graaf** has been a staff member of the Department of Electrical Engineering of the Delft University of Technology since 1976. He received his BSEE degree in Electrical- and Control Engineering from the Technische Hogeschool in Rotterdam in 1983. Currently he is working on electronic circuits for silicon sensors.

**Karin Hedsten** received her PhD from Chalmers University of Technology in 2009. Her research interest areas are MEMS/MOEMS, micro-optics fabrication, and bio applications. She is currently with the Nano-Fabrication Laboratory at Chalmers University of Technology.

**Peter Enoksson** graduated with an M.Sc. in Engineering Physics in 1986. After working for a time he returned to his studies and received a Licentiate of Engineering in 1995 and a PhD in 1997 from the Royal Institute of Technology (KTH) in Stockholm. In 1997, he became assistant professor and in 2000 was appointed “docent” at the Department of Signals, Sensors and Systems at KTH. Peter Enoksson was appointed as Professor of Microsystems on October 1, 2001 at Chalmers University of Technology. One of Peter Enoksson’s main research interests is how resonance can be used to enhance performance in MEMS, especially for fluid applications. This has led to devices such as an extremely accurate liquid density/mass-flow sensor, an optically actuated and detected force sensor as well as actuators, such as a pump, all running in resonance. Another of Peter Enoksson’s research orientations is biomedical systems. Examples of this are an electrode developed specially to monitor EEG (brain activity) signals during surgery and a sensitive, low-power accelerometer intended for pacemaker feedback.

**José Higo Gomes Correia** received his PhD in Electrical Engineering in 1999 from Delft University of Technology. He is professor of Department of Industrial Electronics, University of Minho, Portugal. His main research areas are Micromachining and microfabrication technology for mixed-mode systems, Solid-state integrated sensors, microactuators and Microsystems, Analog and digital integrated circuits, Wireless systems for sensors and actuators and Microcomputer-based instrumentation and data-acquisition systems.

**Reinoud F. Wolffenbuttel** received an M.Sc. degree in 1984 and a PhD degree in 1988, both from the Delft University of Technology. Between 1986 and 1993 he has been an assistant professor and since 1993 he has been an associate professor at the Department of Microelectronics, Faculty of Information Technology and Systems of the Delft University of Technology and is involved in instrumentation and measurement in general and on-chip functional integration of microelectronic circuits and silicon sensor, fabrication compatibility issues and micromachining in silicon and microsystems in particular. He was a visitor at the University of Michigan, Ann Arbor, USA in 1992, 1999 and 2001, Tohoku University, Sendai, Japan in 1995 and EPFL Lausanne, Switzerland in 1997. He is the recipient of a 1997 NWO pioneer award. He served as general chairman of the Dutch national sensor conference in 1996, Eurosensors in 1999 and Micromechanics Europe in 2003.